

ChemComm

Accepted Manuscript



This is an *Accepted Manuscript*, which has been through the Royal Society of Chemistry peer review process and has been accepted for publication.

Accepted Manuscripts are published online shortly after acceptance, before technical editing, formatting and proof reading. Using this free service, authors can make their results available to the community, in citable form, before we publish the edited article. We will replace this *Accepted Manuscript* with the edited and formatted *Advance Article* as soon as it is available.

You can find more information about *Accepted Manuscripts* in the [Information for Authors](#).

Please note that technical editing may introduce minor changes to the text and/or graphics, which may alter content. The journal's standard [Terms & Conditions](#) and the [Ethical guidelines](#) still apply. In no event shall the Royal Society of Chemistry be held responsible for any errors or omissions in this *Accepted Manuscript* or any consequences arising from the use of any information it contains.

COMMUNICATION

Filamentous Supramolecular Peptide-Drug Conjugates as Highly Efficient Drug Delivery Vehicles

Cite this: DOI: 10.1039/x0xx00000x

Miao Yang,^{†a} Dawei Xu,^{†a} Linhai Jiang,^a Lin Zhang,^b Derek Dustin,^a Reidar Lund,^c Ling Liu^b and He Dong^{*a}

Received 00th January 2012,

Accepted 00th January 2012

DOI: 10.1039/x0xx00000x

www.rsc.org/

We report here a facile approach to prepare filamentous supramolecular peptide-drug conjugates with precise drug/carrier stoichiometry, nearly 100% loading efficiency and exceptional anti-cancer drug efficacy for chemotherapy.

Control over drug loading, composition and overall morphology of drug delivery vehicles is crucial for their proper function in chemotherapy.¹ Compared to spherical particles, filamentous nanocarriers demonstrated longer circulating half-life² and improved vascular targeting.³ Organic filamentous particles are mostly formed through the self-assembly of amphiphilic block-copolymers⁴ and amphiphilic peptides⁵ with suitable hydrophobic/hydrophilic ratio to form cylindrical micelles. These micelles have a typical length in the order of micrometers and have extended circulation half-life under fluid flow conditions. However, the cellular uptake of the elongated structures was found to be less efficient compared to that of spheres.⁶ For systemic therapeutics delivery, there is a great need to develop cylindrical drug carriers with a smaller dimension to meet the structural requirements for efficient tumor penetration and cellular uptake.⁷ Equally important is the control over drug loading capacity and efficiency. Formulation through physical encapsulation of hydrophobic drugs unintentionally increases the hydrophobic volume and may change the molecular packing parameter of the amphiphile. As a consequence, the morphology of the nanocarriers, drug loading capacity and efficiency may vary from batch to batch depending on the formulation methods.

To address these challenges, we set out to prove our design of covalent drug-peptide-PEG conjugates and their self-assembly into filamentous supramolecular peptide-drug conjugates. The supramolecular scaffold is based on the previously designed multidomain peptides (MDPs) which form short, soluble nanofibers through the balance of multiple attractive intermolecular forces and electrostatic repulsions.⁸ Current work demonstrated that these supramolecular polymers can be used as scaffolds to append hydrophobic anticancer drugs without severely affecting the size and morphology of the nanofibers. Peptide-drug conjugates have been used for the delivery of anti-cancer drugs. It was until recently that

Cui's group reported on the self-assembly of a peptide-drug conjugate, termed as drug amphiphiles into supramolecular nanostructured materials.^{5e,9} The hydrophobic interactions between drug molecules drive the self-assembly of the conjugate into filamentous supramolecular nanostructures with therapeutic agents buried inside the nanostructure. Inspired by the concept of supramolecular anticancer drug assembly, our design provides an alternative strategy to assemble drugs at more solvent accessible sites on a filamentous supramolecular polymer. Such architecture could allow for rapid release of therapeutics from the delivery vehicles without overcoming significant steric hindrance and diffusion barrier upon the application of specific stimuli. We will demonstrate that the overall nanostructure of the assembly is largely dictated by the peptide-peptide interactions, rather than the physical and chemical property of the therapeutic agents used in the study. To certain extent, this will help alleviate the concern of batch-to-batch structural variation during pharmaceutical formulation where drug-drug interactions are important factors in terms of structural and chemical composition control. We will herein demonstrate and prove such design principles of supramolecular polymer-drug conjugates and their exceptional *in vitro* therapeutics delivery efficacy.

In this work, K₂(QL)₆K₂ (MDP26), a beta sheet forming peptide, was selected as the supramolecular polymer precursor to form soluble nanofibers. PEG (MW=750Da) was attached at the N-terminus of MDP26 to improve the solubility of the drug-peptide conjugate in aqueous solution. As demonstrated by circular dichroism (CD) spectroscopy, both PEGylated and non-PEGylated peptides showed a characteristic of beta sheet structure with a minimum absorption at 216 nm. (Fig. S1) Transmission Electron Microscopy (TEM) clearly showed the formation of short fibers upon PEG conjugation (Fig. S2a). Solution small angle X-ray scattering (SAXS) analysis using a simplistic scattering model of sheets with Gaussian chains on the sides was performed.¹⁰ The results showed that both MDP26 and MDP26-PEG750 form fibers with inner diameter of 6-7 nm, a height of 4 nm and lengths larger than c=40-50 nm. (Fig. S3) These filaments were covered with PEG chains at each side (along the c-axis) having dimensions in terms of the radius of gyration, R_g=0.7 nm.

Hydroxycamptothecin (HCPT) was used as a model hydrophobic anticancer drug and conjugated on both MDP26 and MDP26-PEG. The chemical structure and the self-assembly of the HCPT-MDP26-PEG conjugate was shown in **Fig. 1**.

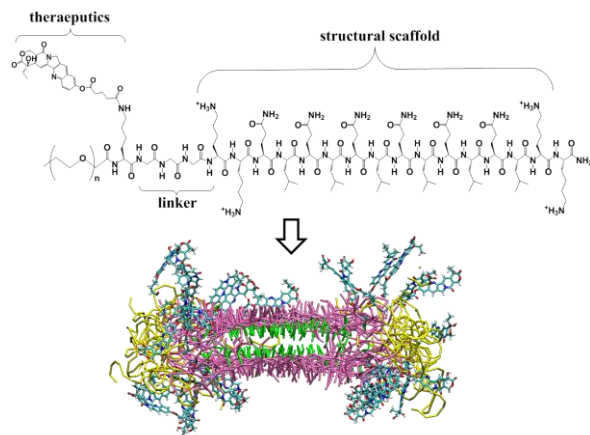


Fig. 1 Chemical structure of the drug-peptide-PEG conjugate and its self-assembly into supramolecular peptide-drug conjugates. Sticks chemical structure: HCPT. Yellow: PEG shell flanking the peptide-based supramolecular polymer backbone to protect intermolecular aggregation of HCPT. Purple: the side chain of the hydrophilic residues. Green: the side chains of the hydrophobic residues.

Without PEG attachment, the assembly of HCPT-MDP26 could proceed to form either nanofibers or cylindrical micelles as shown in **Fig. S4**. The supramolecular assembly is dictated by an energetic competition between the formation/rupture of hydrogen bonds in MDP26 and the exposure/shielding of the hydrophobic HCPT to/from aqueous solvents. The fiber configuration satisfies the hydrogen bonds among MDP26 while sacrificing the hydrophobic packing of HCPT. The cylindrical micelle has HCPT shielded from aqueous solvents, but disrupts the intermolecular hydrogen bonding among MDP26. For cylindrical micelles, incorporating charged lysine residues in the interfacial region can increase the energy penalty as well. Fibers and cylindrical micelles can be differentiated through TEM studies where nanofiber has a diameter close to the length of a single peptide chain in a stretched beta sheet conformation (~ 6.8 nm corresponding to 16 aa plus 3 glycine linker), while the diameter of a cylinder doubles. As shown in **Fig. 2a**, it is very rare to observe individual cylinders with diameters above 14 nm. Rather, most of the nanostructures showed a diameter of 7-8 nm corresponding to the nanofiber configuration. Molecular dynamic simulations have been performed with 120 HCPT-MDP26 molecules assembled in the fiber and cylindrical micelle forms, respectively. Both systems contain 11520 HCPT-MDP26 atoms/beads and 107052 water molecules. Results showed that the potential energy of fiber is 9866.5 kJ/mol lower than that of the cylindrical micelles, implying that the energetic gain associated with hydrogen bonds exceeds the energy loss due to water exposure, and packing into fiber is more energetically favorable for HCPT-MDP26. More systematic simulation studies are currently underway and will be reported separately.

The preservation of fibrous structure is quite impressive given the strong hydrophobicity of HCPT which often leads to instantaneous nanoprecipitation of drug-polymer conjugates in the form of spherical nanostructures. Such observation clearly justifies the strength of the non-covalent inter-molecular interactions among peptides to maintain the filamentous nanostructure despite the presence of other competing interactions. Therefore, we believe that peptide-peptide interaction can be used as another key parameter to

tune the nanostructure and stability of the supramolecular peptide-drug conjugates as the size and hydrophobicity of drug molecules vary. The stabilization effect of PEG on nanostructure is obvious. Without PEG, large fractions of materials aggregated although fiber morphology is still visible. The addition of PEG significantly improved the solubility of HCPT-MDP26 and dramatically minimized fiber aggregation. TEM showed individually dispersed fibers with an average diameter of ~ 8 nm and average length of 50 ± 10 nm (**Fig. 2b** and **Fig. S5** for statistical length measurements).

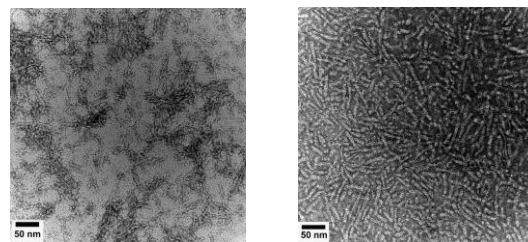


Fig. 2 Negatively stained TEM images of (a) HCPT-MDP26 and (b) HCPT-MDP26-PEG. Peptide concentration: 100 μ M in Tris buffer (pH 7.4, 20 mM).

When MDP26 and its derivatives self-assemble, positively charged interfaces are formed due to the presence of lysine residues at both termini. The cationic nature makes these materials more susceptible to non-specific serum protein binding.¹¹ We set out to test the serum stability using a fluorescein labelled MDP26-PEG conjugate, termed as FAM-MDP26-PEG. Fluorescein serves dual roles as both a fluorescence reporter and a hydrophilic drug analogue. FAM-MDP26-PEG formed similar fibrous structure to the HCPT conjugate. (**Fig. S6**) We have previously established a fluorescence self-quenching and recovery method for the evaluation of the kinetic stability of amphiphilic micelles in the presence of bovine serum albumin (BSA).¹² The same principle and experimental setup was used here to quantify the rate of monomer dissociation from the supramolecular fibrous assembly. **Fig. S7** shows the fitting of the fluorescence recovery data into first-order dissociation kinetics, giving rise to a dissociation rate constant at 0.00317 hr^{-1} in FBS and $0.0045363 \text{ hr}^{-1}$ in BSA, corresponding to half-lives of 9 days and 6 days, respectively. Although some approximation in the calculation of the half-life and of course more complex biological environment during *in vivo* blood circulation, the exceptional stability demonstrated by the supramolecular structured peptide is unprecedented. The enhanced kinetic stability is presumably attributed to the presence of intermolecular hydrogen bonding and hydrophobic interactions between the beta-sheet forming peptide backbone which provides exceptional structural integrity and stability.

Cytotoxicity of peptides and drug-peptide conjugates was assessed in HepG2 human hepatocellular carcinoma for which HCPT showed moderate toxicity compared to other cancer cell lines such as breast cancer cells, MCF-7.¹³ Peptides and drug-peptide conjugates were incubated with HepG2 cells for 48 hours followed by CCK8 cytotoxicity assay. Despite the large population of the positive charges, supramolecular peptides alone demonstrated negligible cytotoxicity. (**Fig. S8**) The drug conjugate, HCPT-MDP26-PEG showed a dose-dependent cytotoxicity with an IC_{50} of 1.27 μ M, comparable to the IC_{50} of free HCPT at $\sim 1.3 \mu$ M. (**Fig. 3a**) At high drug dosage, the drug conjugate is much more potent than free HCPT. To further understand the enhanced drug efficacy of the fiber-forming drug conjugates, a control peptide MDP24 (sequence: $\text{K}_2(\text{QL})_4\text{K}_2$) was synthesized as a structural analogue of MDP26, and used for drug conjugation. HCPT-MDP24-PEG is highly soluble, but did not self-assemble into supramolecular structures in aqueous buffer (Tris, pH=7.4, 20mM) as shown by TEM (data not shown) while CD showed a random coil secondary structure. (**Fig. S1**) The

cytotoxicity of HCPT-MDP24-PEG is significantly lower than that of both HCPT-MDP26-PEG and free HCPT. Two factors may contribute to the difference of cytotoxicity, i. e. cellular uptake and drug release kinetics. Fluorescently labelled MDP26-PEG showed much higher cellular uptake than that of MDP24-PEG as demonstrated by both confocal microscopy (Fig. 3b and 3d) and flow cytometry (Fig. 3c). Drug release rate was found to be faster for the fiber-forming drug conjugates than that of single chain peptide-drug conjugate. (Fig. S9) Studies have shown that the hydrophilicity of surrounding drug molecules can be a major driving force to affect ester hydrolysis rates.¹⁴ The difference of drug release kinetics observed here may be attributed to the difference of drug microenvironment. A more hydrophilic microenvironment is created for HCPT-MDP26-PEG nanofiber where drugs are surrounded by high populations of charged lysine residues and polar glutamine residues, whereas drug may be less accessible for hydrolysis in HCPT-MDP24-PEG. It is worth to note that current system serves as a model system to demonstrate the concept of supramolecular assembly of MDP-drug conjugates and their *in vitro* anticancer drug efficacy. The release kinetics of drug molecules can be further tuned to suit *in vivo* applications by using different linker chemistry between peptides and drug molecules.¹⁵

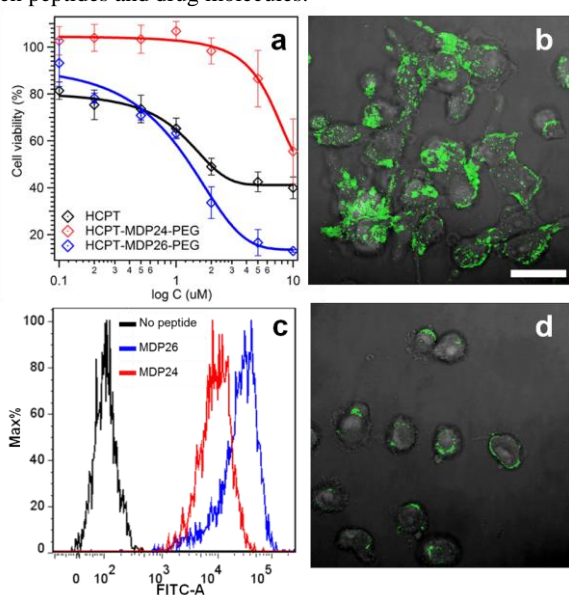


Fig. 3 (a) Cell viability of free HCPT, HCPT-MDP26-PEG and HCPT-MDP24-PEG after 48 hours incubation with HepG2 cells. (b) Cellular uptake of FAM-MDP26-PEG and (c) FAM-MDP24-PEG examined by confocal microscopy. The images shown are the overlay of the image under bright field and fluorescence excited at 488 nm. Scale bar: 30 μm . (d) Cellular uptake of FAM-MDP26-PEG and FAM-MDP24-PEG evaluated by flow cytometry.

In conclusion, we have demonstrated a new design of filamentous supramolecular peptide-drug conjugate which showed desired properties as therapeutics delivery vehicles, including high drug density and serum stability, precisely controlled drug/carrier loading stoichiometry, nearly 100% loading efficiency and exceptional anticancer drug efficacy. Understanding the self-assembly of the supramolecular peptide-drug conjugate will help build up a solid foundation for the rational design of supramolecular nanostructured materials, in particular nanofiber-based materials as long-circulating nanocarriers for a range of biomedical applications, not limited to drug delivery. They can be potentially useful for vaccine delivery and antimicrobial materials design and development, all of which require advanced control over nanostructure.

Clarkson University is acknowledged for support of this work. We acknowledge the Biology Department at St. Lawrence University for

confocal microscopy imaging and Trudeau institute for the help on flow cytometry quantification. EMBL, Hamburg is acknowledged for allocation of the beamtime at the bioSAXS P12 instrument, Petra III. We thank Dr. Petr. Konarev for the help on SAXS experiments.

Notes and references

^a Department of Chemistry and Biomolecular Sciences, Clarkson University, Potsdam, NY, US 13699.

^b Department of Mechanical and Aerospace Engineering, Utah State University, Logan, UT, US 84322

^c Department of Chemistry, University of Oslo, Postboks 1033 Blindern, 0315 Oslo, Norway.

E-mail: hdong@clarkson.edu

†Electronic Supplementary Information (ESI) available: peptide synthesis, experimental procedures, HPLC, masspec, TEM, CD, fluorescence and kinetics fitting. See DOI: 10.1039/c000000x/

‡ These authors contribute equally to this work.

1 (a)R. Duncan, *Nat. Rev. Cancer*, 2006, **6**, 688; (b)N. Nishiyama and K. Kataoka, *Pharmacol. Ther.*, 2006, **112**, 630; (c)J. Shi, A. R. Votruba, O. C. Farokhzad and R. Langer, *Nano Lett.*, 2010, **10**, 3223; (d)V. P. Torchilin, *Nat. Rev. Drug Discov.*, 2005, **4**, 145; (e)M. Ferrari, *Nat. Rev. Cancer*, 2005, **5**, 161; (f)R. Tong and J. Cheng, *Polym. Rev.*, 2007, **47**, 345.

2 (a)Y. Geng, P. Dalhaimer, S. Cai, R. Tsai, M. Tewari, T. Minko and D. E. Discher, *Nat. Nanotechnol.*, 2007, **2**, 249; (b)N. Nishiyama, *Nat. Nanotechnol.*, 2007, **2**, 203; (c)J.-H. Park, G. von Maltzahn, L. Zhang, M. P. Schwartz, E. Ruoslahti, S. N. Bhatia and M. J. Sailor, *Adv. Mater.*, 2008, **20**, 1630.

3 P. Kolhar, A. C. Anselmo, V. Gupta, K. Pant, B. Prabhakarparandian, E. Ruoslahti and S. Mitragotri, *Proc. Nat. Acad. Sci. U.S.A.*, 2013.

4 (a)S. Jain and F. S. Bates, *Science*, 2003, **300**, 460; (b)Q. Ma, E. E. Remsen, C. G. Clark, T. Kowalewski and K. L. Wooley, *Proc. Nat. Acad. Sci. U.S.A.*, 2002, **99**, 5058; (c)R. C. Hayward and D. J. Pochan, *Macromolecules*, 2010, **43**, 3577.

5 (a)A. Trent, R. Marullo, B. Lin, M. Black and M. Tirrell, *Soft Matter*, 2011, **7**, 9572; (b)D. J. Toft, T. J. Moyer, S. M. Standley, Y. Ruff, A. Ugolkov, S. I. Stupp and V. L. Cryns, *ACS Nano*, 2012, **6**, 7956; (c)H. R. Marsden, A. V. Korobko, E. N. M. van Leeuwen, E. M. Pouget, S. J. Veen, N. A. J. M. Sommerdijk and A. Kros, *J. Am. Chem. Soc.*, 2008, **130**, 9386; (d)Y.-b. Lim and M. Lee, *J. Mater. Chem. B*, 2008, **18**, 723; (e)A. G. Cheetham, P. Zhang, Y.-a. Lin, L. L. Lock and H. Cui, *J. Am. Chem. Soc.*, 2013, **135**, 2907.

6 K. Zhang, H. Fang, Z. Chen, J.-S. A. Taylor and K. L. Wooley, *Bioconjugate Chem.*, 2008, **19**, 1880.

7 (a)A. I. Minchinton and I. F. Tannock, *Nat. Rev. Cancer*, 2006, **6**, 583; (b)S. E. A. Gratton, P. A. Ropp, P. D. Pohlhaus, J. C. Luft, V. J. Madden, M. E. Napier and J. M. DeSimone, *Proc. Nat. Acad. Sci. U.S.A.*, 2008, **105**, 11613.

8 H. Dong, S. E. Paramonov, L. Aulisa, E. L. Bakota and J. D. Hartgerink, *J. Am. Chem. Soc.*, 2007, **129**, 12468.

9 R. Lin, A. G. Cheetham, P. Zhang, Y.-a. Lin and H. Cui, *Chemical Communications*, 2013, **49**, 4968.

10 Y. Yan, A. de Keizer, A. A. Martens, C. L. P. Oliveira, J. S. Pedersen, F. A. de Wolf, M. Drechsler, M. A. Cohen Stuart and N. A. M. Besseling, *Langmuir*, 2009, **25**, 12899.

11 J. Svenson, B.-O. Brandsdal, W. Stensen and J. S. Svendsen, *J. Med. Chem.*, 2007, **50**, 3334.

12 H. Dong, J. Y. Shu, N. Dube, Y. Ma, M. V. Tirrell, K. H. Downing and T. Xu, *J. Am. Chem. Soc.*, 2012, **134**, 11807.

13 (a)J. Wang, R. Wang and L. B. Li, *J. Colloid Interface Sci.*, 2009, **336**, 808; (b)C. Xie, X. Li, X. Luo, Y. Yang, W. Cui, J. Zou and S. Zhou, *Int. J. Pharm.*, 2010, **391**, 55.

14 Y. S. Jo, J. Gantz, J. A. Hubbell and M. P. Lutolf, *Soft Matter*, 2009, **5**, 440.

15 E. A. Dubikovskaya, S. H. Thorne, T. H. Pillow, C. H. Contag and P. A. Wender, *Proc. Nat. Acad. Sci. U.S.A.*, 2008, **105**, 12128.